Steep dip Kirchhoff migration for linear velocity gradients

Maria Donati, Nicolas B. Martin, and John C. Bancroft

ABSTRACT

A linear-with-depth velocity function is a typical assumption in clastic basins of Tertiary-Quaternary origin sometimes associated with salt domes.

In this case, the raypaths can be approximated by arcs of circles with spherical wavefronts. The 2D Kirchhoff summation curve is no longer valid for large offsets and steep dips. It then becomes neccesary to consider a non-hyperbolic summation curve for proper time imaging of dips up to and beyond 90° for these "turning" zero-offset sections.

A non-hyperbolic summation curve, based in a 8th order polinomial equation, is used to image 120° dipping events. It is applied to synthetic zero-offset sections generated by turning-ray modelling on depth models including a diffractor point and a 2-D sphere.

INTRODUCTION

The basic theory of the turning-ray modeling assumes that when the velocity field is linear-with-depth, $V = V_0(1+kz)$, the resultant theoretical raypaths are arcs of circles (Hagedoorn, 1954; Kleyn,1983, Richardson, 1992) defined by

$$\left(x-\cot\left(\frac{\theta_0}{k}\right)\right)^2+\left(z-\left(\frac{-1}{k}\right)\right)^2=\left(\csc\left(\frac{\theta_0}{k}\right)\right)^2 \qquad (1)$$

Where θ_0 represents the initial angle of the raypath from the vertical as it leaves the source, x is the horizontal distance between the source-reflector point spent by the turning ray and z_0 is the depth of the reflector point. The traveltime along such an arc at a reflector depth $z= z_0$ is given by

$$T=\left(\frac{1}{kV_0}\right)\left[\ln\left(\tan\left(\frac{\theta}{2}\right)\right)-\ln\left(\tan\left(\frac{\theta_0}{2}\right)\right)\right] \qquad (2)$$

Where

$$\theta=\arcsin\left((1+kz_0)\sin\theta_0\right) \qquad (3)$$

represents the incident angle of the raypath when it reachs the reflector as illustrated in Fig. 1a.

Both expressions can be used to estimate the two-way travel time associated with a given CMP for normal incidence reflections in a linear velocity medium. The relation between dip and θ for normal incidence on a sphere is shown in Fig. 1b. By knowing the depth model it is easy to define the dip and angle θ at each point on the reflector. Then given the gradient k and depth z_0, θ_0 and travel time T can be determined by eqs. (2-3).

The resultant t-x bending curves for a diffractor point buried at two different depths 1,500 m and 4,000 m, with an initial velocity V_0 = 1,600 m and a gradient k = $0{,}3/V_0$, are shown in Figs. 2a, b.

From both pictures it is evident that for the shallower diffractor offsets up 5,000 m are necessary for recording dips up to 90°, while the deeper one requires offsets up 10,000 m. In contrast, the offsets required for recording the same dips without bending effect are two times higher than the former ones. In other words, the linear velocity gradient reduces the maximum offset range for recording steeper dips.

The Figs. 2a, b shows other important fact related to Kirchhoff time migration when a linear gradient is present. The basic assumption in the post-stack Kirchhoff migration is to sum seismic amplitudes on a zero-offset section along a hyperbolic summation curve and to put the summed amplitude at its apex as one migrated sample (Yilmaz, 1987) . The conventional expression for this summation curve is given by

$$T^2 = T_0^{\,2} + 4\left(\frac{h}{V_{rms}}\right)^2 \tag{4}$$

where T_0 is equal to $2\left(z_0/V_{rms}\right)$, h is the half-offset, z is the reflector depth, V_{rms} is the rms velocity at the apex.

For a linear gradient velocity medium the rms velocity is given by

$$V_{rms}^2 = \left(\frac{V_0}{2kT_0}\right)\exp(2V_0kT_0 - 1) \tag{5}$$

where T_0 is the vertical two-way time.

The hyperbolic summation curve is not valid for imaging steeper dips. In fact, the hyperbolic approach may only be valid for dips up to 50°. A non-hyperbolic summation curve, similar to the t-x bending curve of the diffractors in Fig. 2a and b, would enable migration of steeper dips.

This non-hyperbolic curve can be obtained with the least-square curve fitting method for a array of values (x,t) that define a given diffraction curve. Fig. 3 shows this curve fitting for three diffractors at different depths; it is apparent that this approximation is valid for dip up to 120° and offset values to 25,000 m, respectively.

The non-hyperbolic Kirchhoff summation curve (Fig. 4) can be expressed as

$$T^2_{nhyp} = T^2_0 + 4\left(\frac{h}{V_{rms}}\right)^2 - A\left(\frac{h}{V_{rms}}\right)^4 + B\left(\frac{h}{V_{rms}}\right)^6 + C\left(\frac{h}{V_{rms}}\right)^8 \quad (6a)$$

$$A = 0.0765625(kV_0)^2 \quad (6b)$$

$$B = 0.0052843(kV_0)^4$$

$$C = 0.0000902(kV_0)^6$$

ANALYSIS OF RESULTS

Migration of a diffractor point

The first example is a diffractor point buried at z= 200 m with k = $0.5/V_0$ and V_0= 1,600 m/s. The Fig. 5a shows the "zero-offset" bending raypaths associated to dips between 0° - 135°. The stacked section is indicated in Fig. 5b, with a maximum two-way time of 7.5 sec.

The section was migrated using the conventional Kirchhoff summation curve is shown in Fig. 5c. The diffractor point was succesful imaged to a spike at t_0 = 0.245 sec, but these exist "spreading" energy below the spike that couldn't be collapsed by applying this summation curve.

The section was re-migrated with a non-hyperbolic Kirchhoff summation using eq. (6a) and is shown in Fig. 5d. The noisy effect related to the "spreading" energy had been significantly reduced after the application of the approximation given in the eqs. (6a,b).

Migration of a 2-D Sphere

The next depth model is a 2-D sphere of radius 2000 m. with its center burried in a linear velocity medium at a depth z = 2100 m. Zero-offset turning raypaths associated with dips up 120° and the zero offset section are shown in Figs. 6a, b respectively.

The migrated sections obtained by using the hyperbolic and non-hyperbolic Kirchhoff are shown in Figs. 6c and 6d. The hyperbolic results start to deviate at dips beyond 80°, while the non-hyperbolic results show accurate data placewhen up to 120°.

CONCLUSIONS

This article has shown a practical approach to imaging steep reflections on synthetic zero-offset sections by using a direct turning raypath modelling. It is based on the application of a non-hyperbolic summation curve in Kirchhoff time migration. The limitation of conventional hyperbolic summation was shown in a linear velocity gradient medium. A migrated image for dip values up 120° was possible by expanding

the diffraction equation to include terms up to the eight power. The coefficients of the delitional terms were found by least-squared fitting on t-x curves for a diffractor point buried at several depths. The non-hyperbolic summation curve was shown to be valid for a velocity gradient range K between 0.3/Vo and 0.7/Vo, with Vo = 1,600 m/s.

Synthetic examples show that it is possible to migrate dips up to 120° when the difraction shape is computed from equations using offset terms to the eight power while the hyperbolic computation fails for dips over 80°. Both results suggest that the hyperbolic summation curve can't collapse appropriately the energy corresponding to dips greater than 80° in a linear velocity gradient scheme.

ACKNOWLEDGMENTS

We thank Dr. John Bancroft for enlightening discussions and invaluable material support that made possible the development of this article.

REFERENCES

Hagedoorn, J., 1954, A process of seismic reflection interpretation: Geophys. Prosp., 2, 85-127.

Klein, A.H., 1983, Seismic reflection interpretation: Applied Science Publishers LTD.

Richardson, R. P., 1992, Linear velocity function: Reflection times for specific ranges: Geophysics, 57, 1352-1353.

Yilmaz, O., 1987, Seismic data processing: SEG

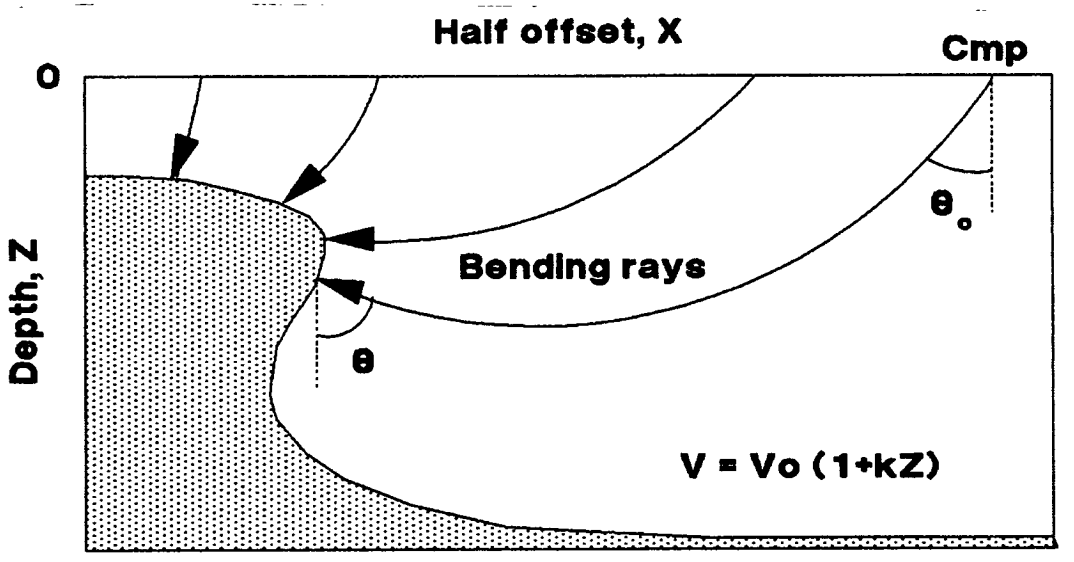

(a)

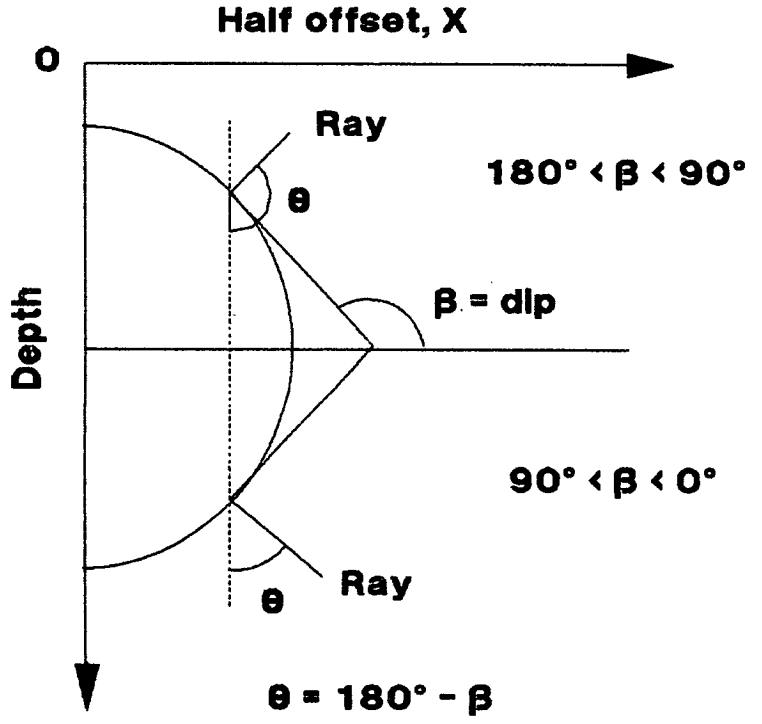

(b)

FIG.1 (a) Turning raypath geometry.
(b) Relation between angle θ and reflector dip β

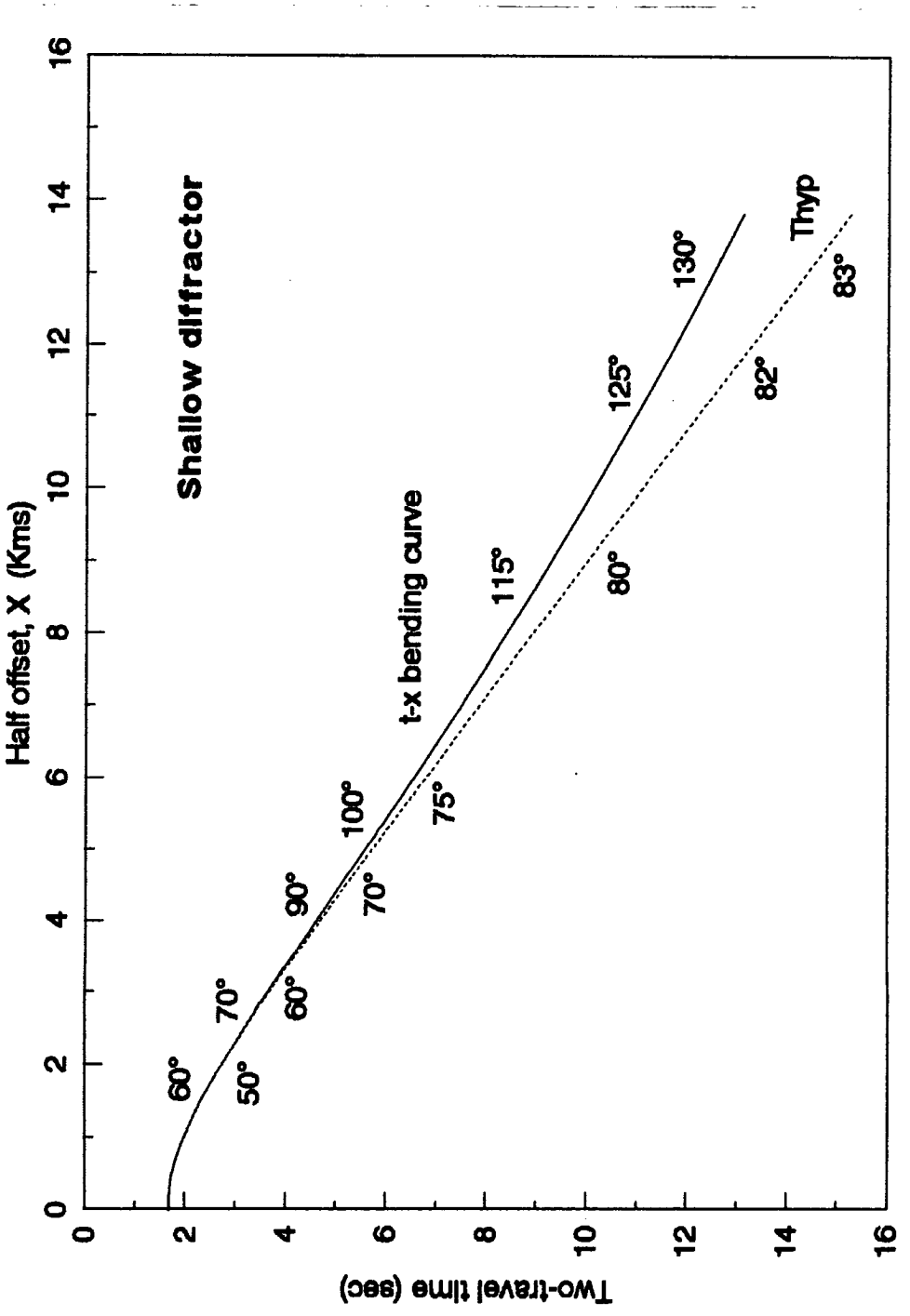

FIG 2a t-x bending and hyperbolic approach curves vs offset value for a diffractor point at a depth z= 1,500 m.

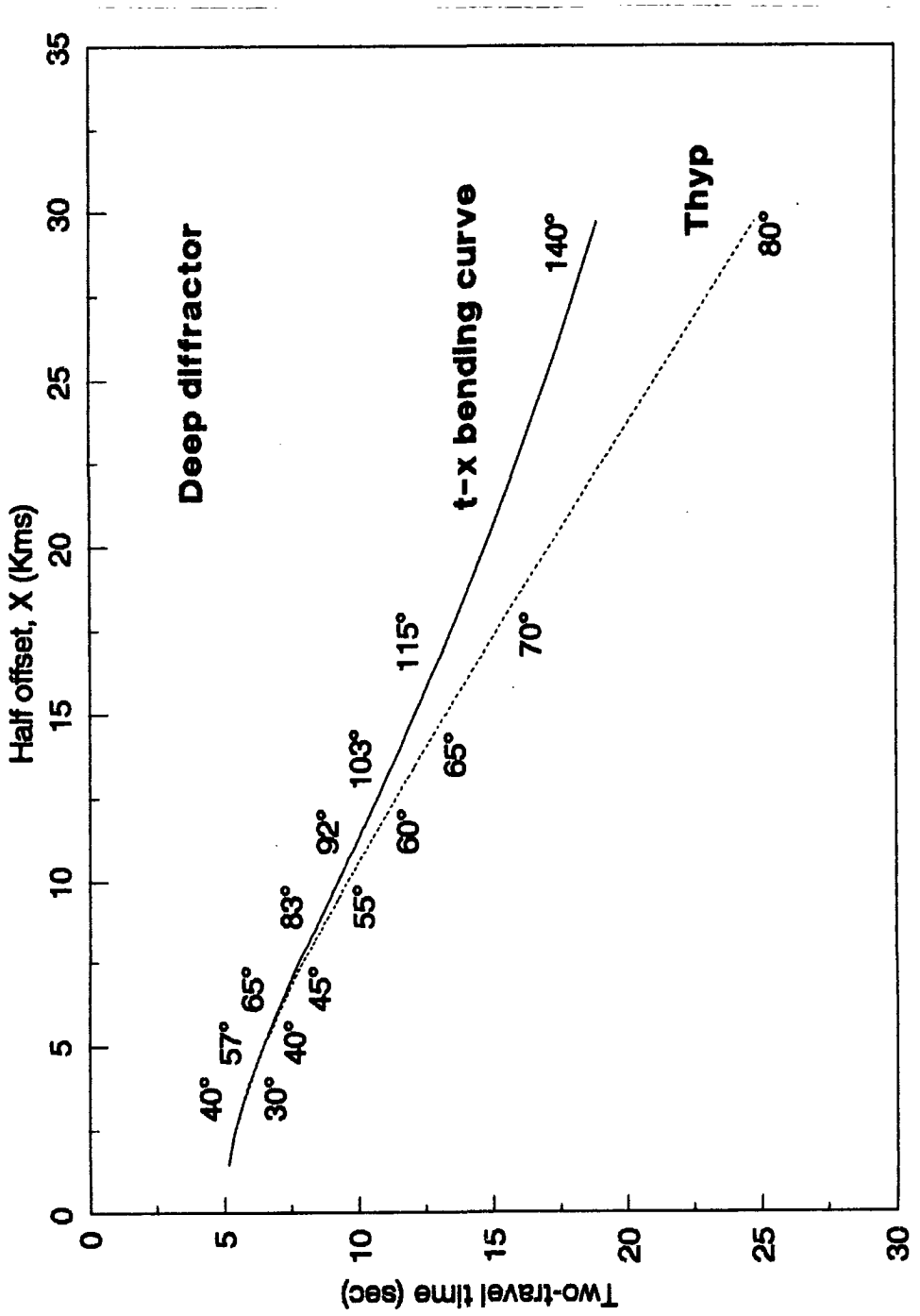

FIG 2b t-x bending and hyperbolic approach curves vs offset for a diffractor point at a depth z= 6,000 m.

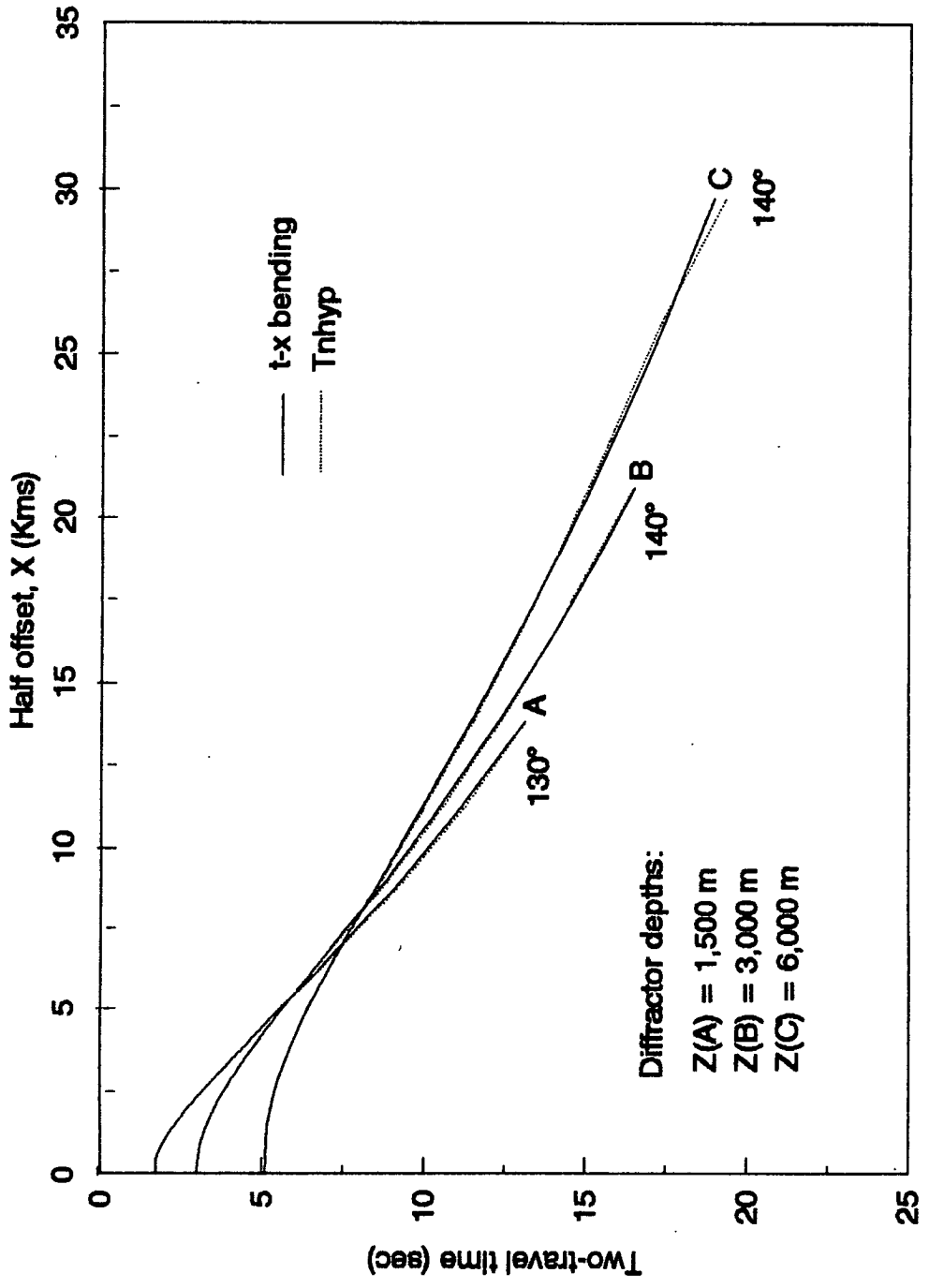

FIG 3 Effect of the depth on the matching between the t-x bending and non-hyperbolic curves for a diffractor point.

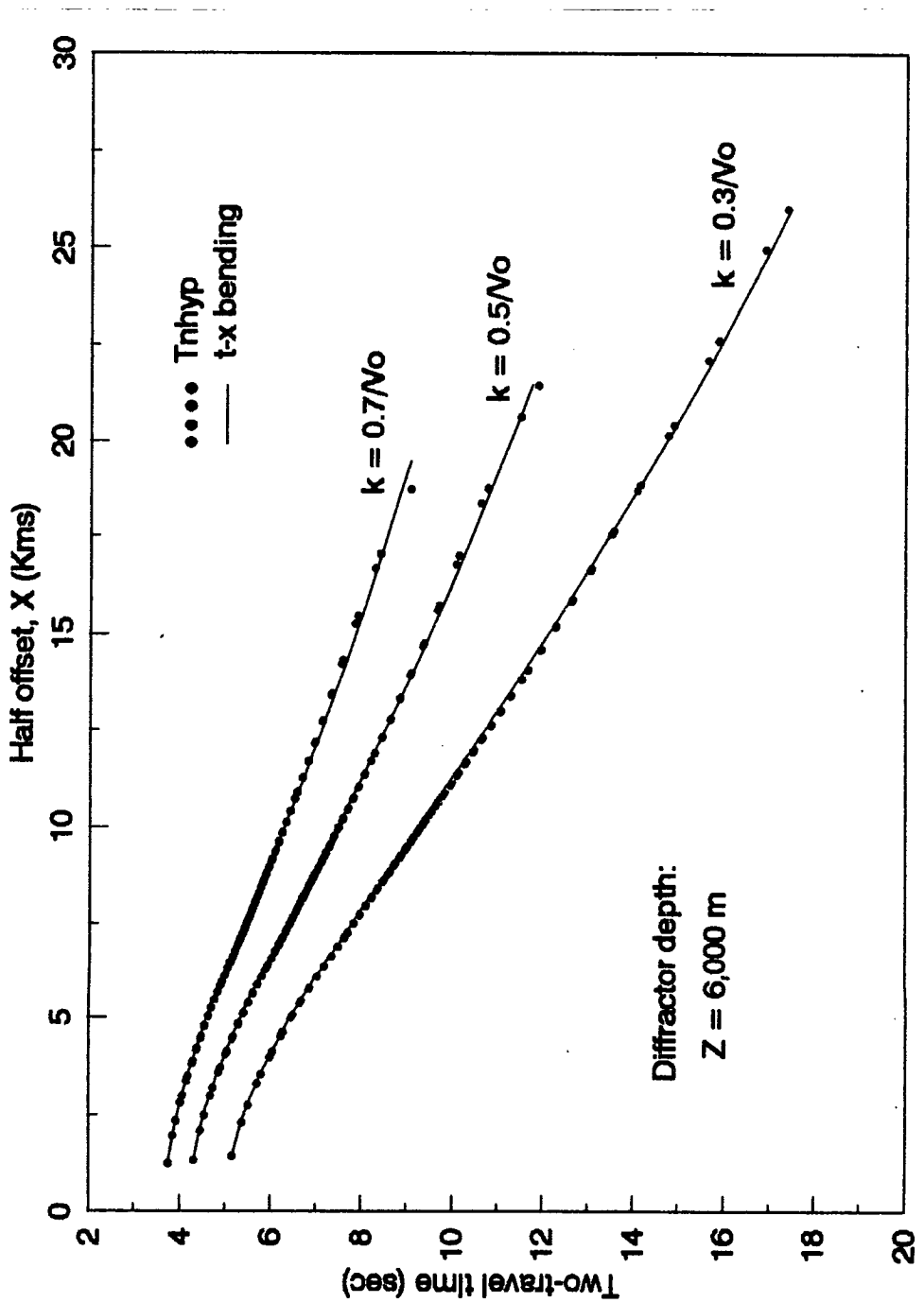

FIG. 4 Effect of the velocity gradient K on the matching between the t-x bending and non-hyperbolic curves for a diffractor point.

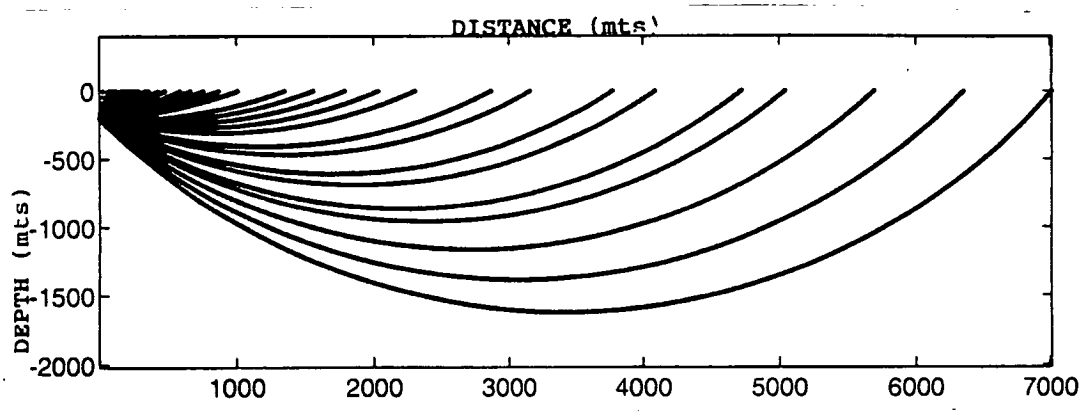

(a)

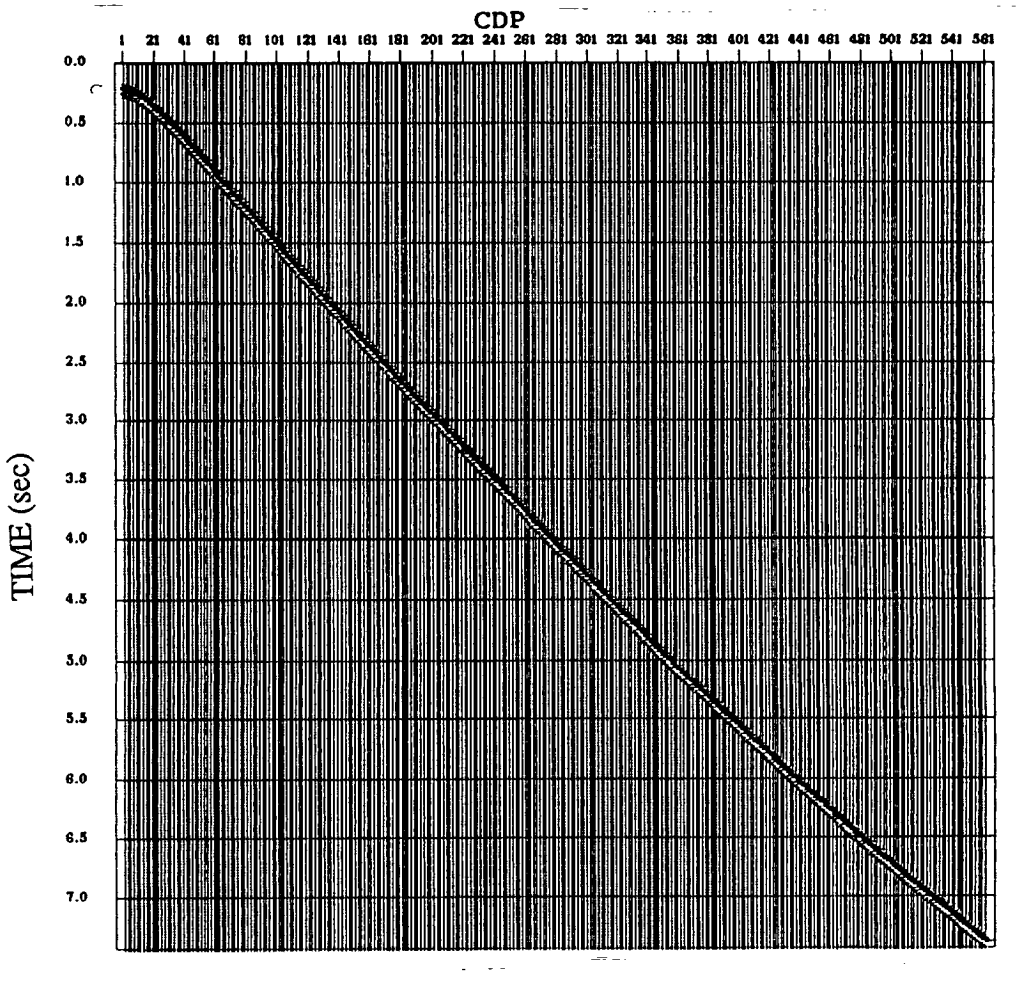

(b)

FIG.5. (a) Turning raypath modelling for a diffractor point burried at a depth z=200m (K= 0.3/V0, V0= 1,600 m/s).
(b) Zero-offset section corresponding to Fig. 5a. Trace spacing 12.5 m.

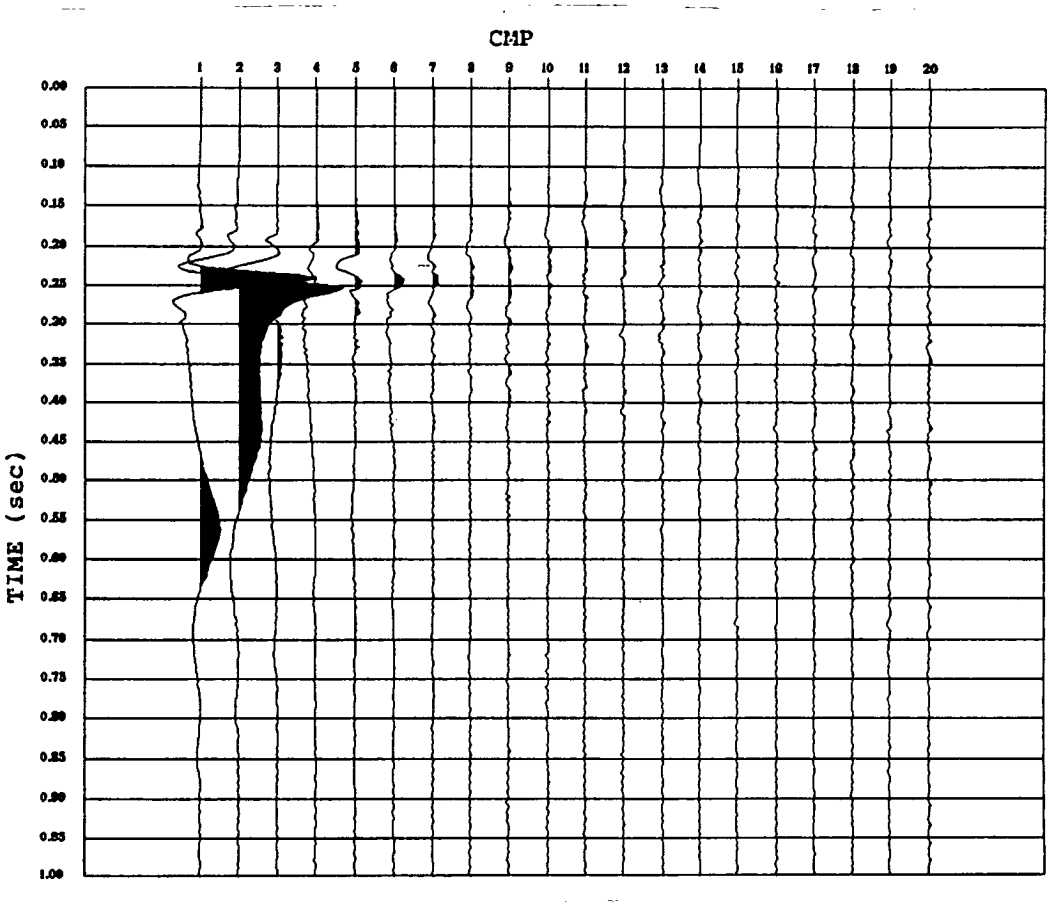

FIG.5c..Kirchhoff time migration with hyperbolic summation curve for the diffractor point in Fig. 5a (K=0.5/V0, V0= 1,600 m/s).

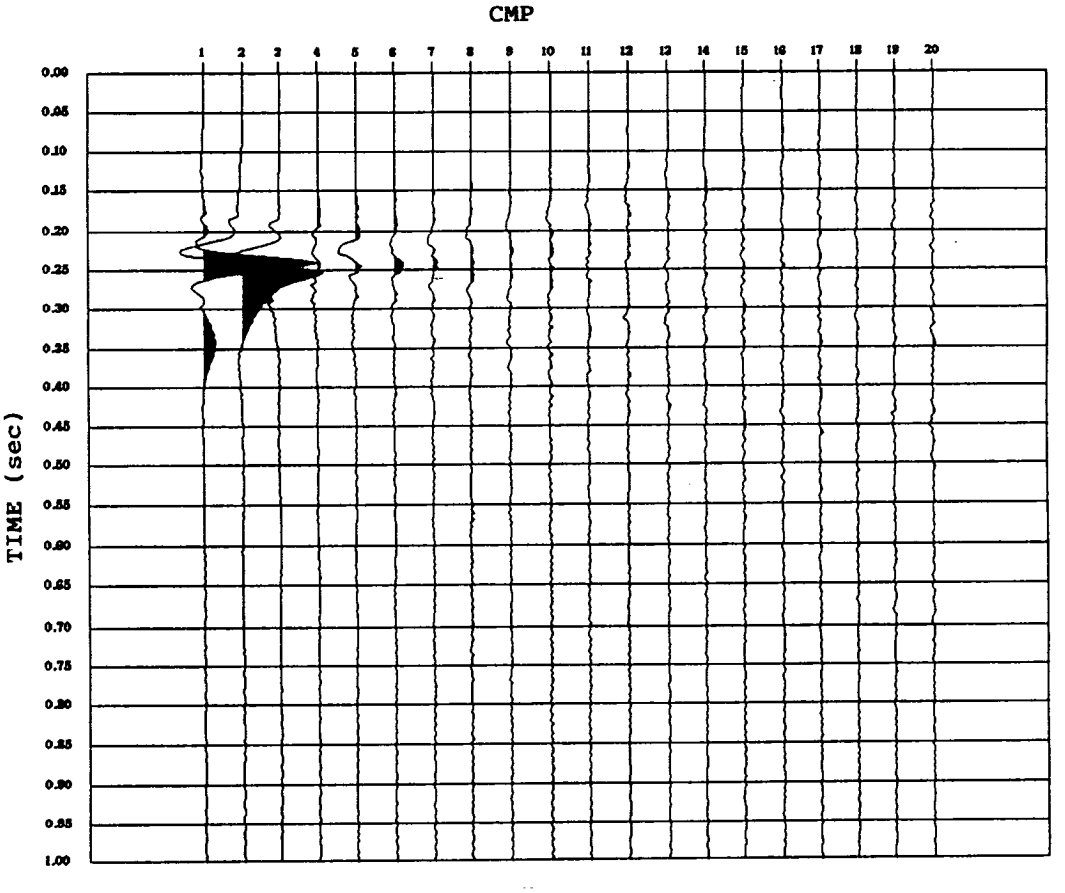

FIG.5d. Kirchhoff time migration with non-hyperbolic summation curve for the diffractor point in Fig. 6a (K= 0.5/V0, V0= 1,600 m/s).

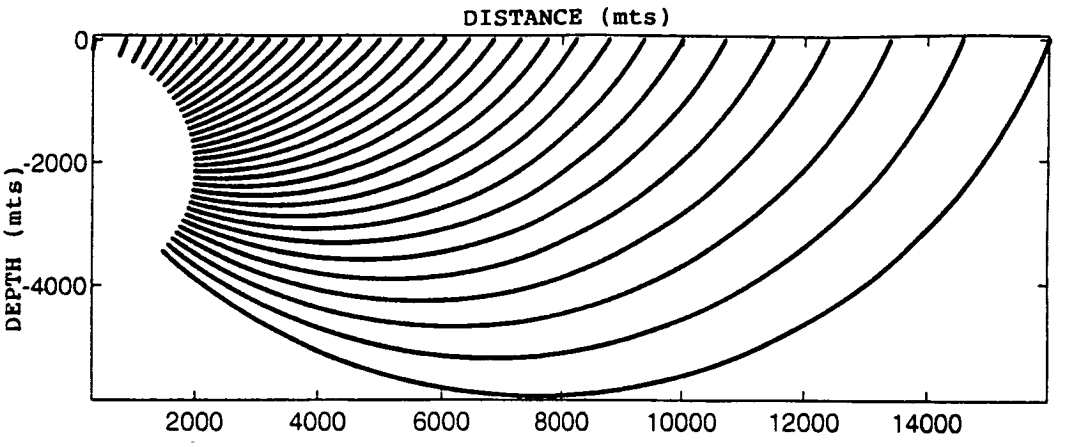

(a)

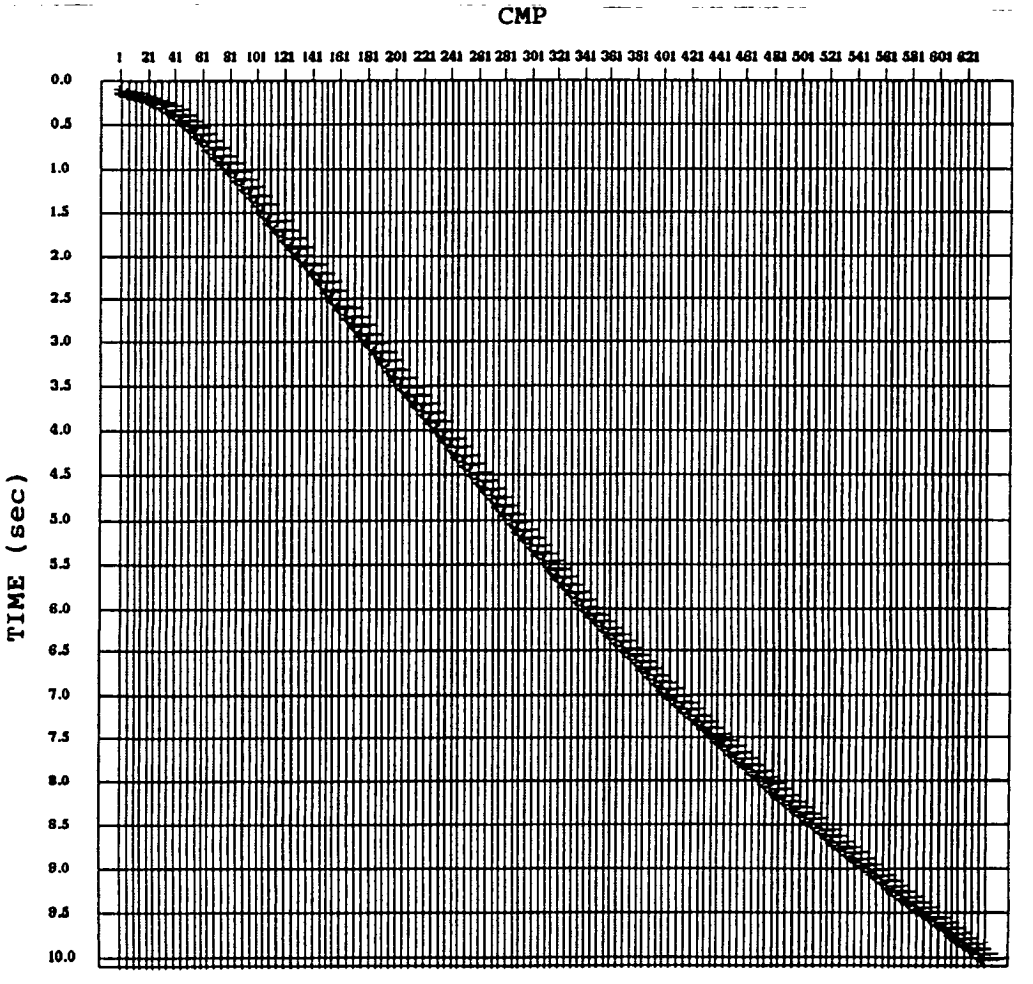

(b)

FIG.6 (a) Turning raypath modelling for a 2-D sphere which center is burried at depth z=2,100m (K=0.5/V0, V0= 1,600 m/s).
(b) Zero-offset section corresponding to Fig. 6a. Trace spacing 25 m.

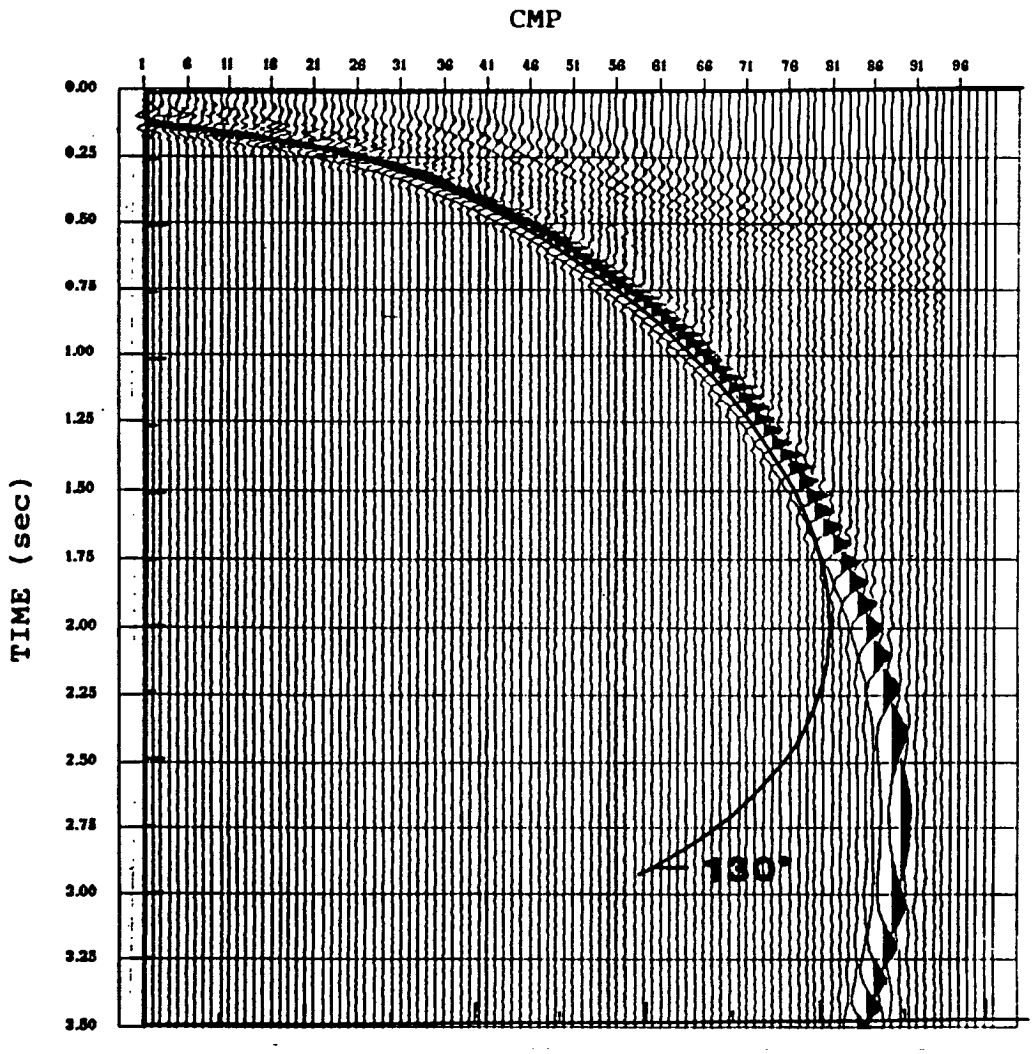

FIG.6c. Kirchhoff time migration with hyperbolic summation curve for the 2-D sphere in Fig. 6a (K= 0.5/V0, V0= 1,600 m/s)..

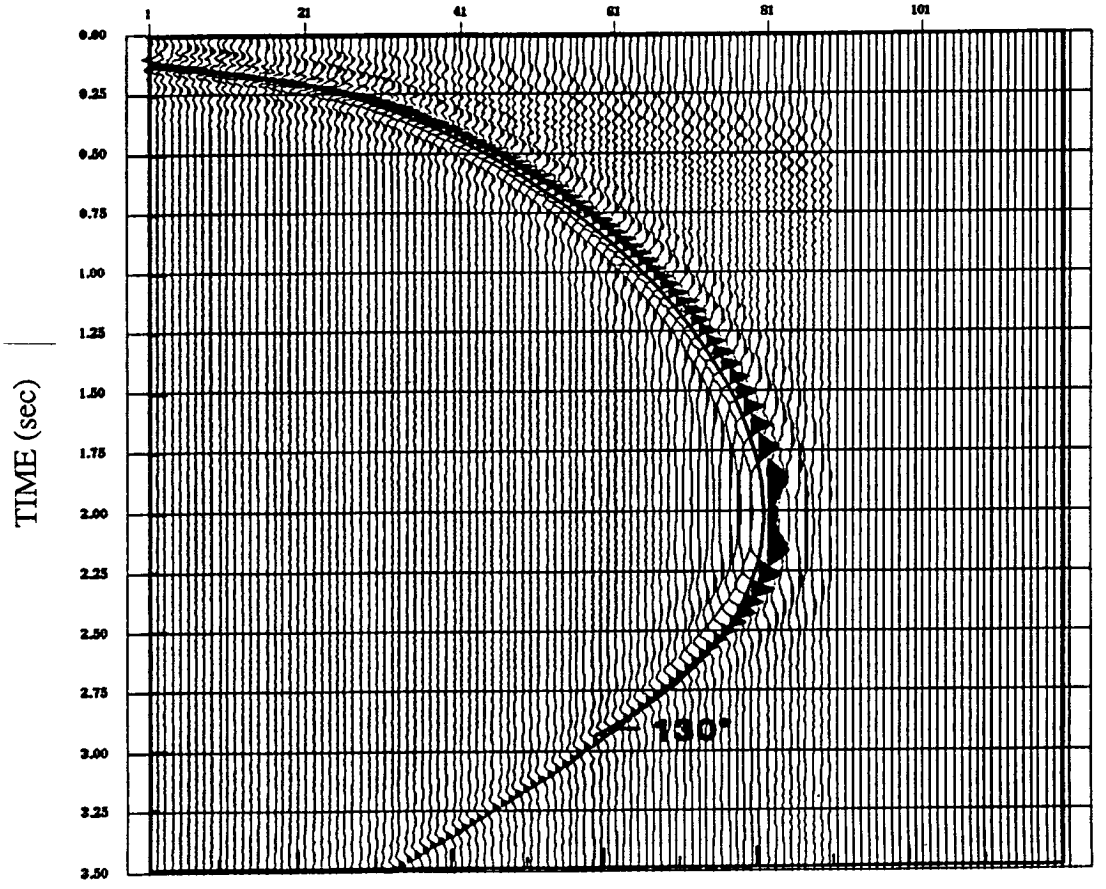

FIG.6d. Kirchhoff time migration with non-hyperbolic summation for the 2-D sphere in Fig. 6a (K=0.5/V0, V0= 1,600 m/s).